Isotope-Filtered 2D NMR of a Protein–Peptide Complex: Study of a Skeletal Muscle Myosin Light Chain Kinase Fragment Bound to Calmodulin

Mitsuhiko Ikura and Ad Bax*

Contribution from the Laboratory of Chemical Physics, National Institute of Diabetes and Digestive and Kidney Diseases, National Institutes of Health, Bethesda, Maryland 20892. Received July 31, 1991

Abstract: An NMR approach is demonstrated for elucidating the conformation of a peptide when tightly bound to a protein. A 26-residue peptide derived from rabbit skeletal muscle myosin light chain kinase, comprising the binding site for calmodulin, was complexed with uniformly (>95%) ^{15}N- and ^{13}C-enriched calmodulin. Improved isotope-filtered two-dimensional NMR techiques were developed for suppressing NMR calmodulin signals. NOE patterns indicate that residues Arg-3 through Ser-21 of the bound peptide form an α-helix. NOE interactions between the peptide and the protein indicate that the N-terminal half of the peptide interacts with the C-terminal domain of calmodulin, and the C-terminal half interacts with the N-terminal calmodulin domain.

Calmodulin (CaM[1]) is a ubiquitous intracellular protein of 148 residues (M_r 16.7 kDa) that plays a key role in coupling Ca^{2+} transients, caused by a stimulus at the cell surface, to events in the cytosol. It performs this role by calcium dependent binding to a host of intracellular enzymes. CaM contains four calcium binding sites of the "EF-hand" type. Its crystal structure[2,3] indicates that the protein consists of two globular domains, each containing two calcium binding sites, connected by a continuous 26-residue α-helix that separates the two globular domains, giving CaM a dumbbell-type structure in the crystalline state. A recent NMR solution study[4] indicates, however, that the so-called "central helix" is disrupted from residue Asp-78 through Ser-81, with a high degree of flexibility in this region of the protein.

Myosin light chain kinase (MLCK) is one of the enzymes that require Ca^{2+} and CaM for activity. It has been shown[5] that CaM binds to residues 577–602 of rabbit skeletal MLCK. A 26-residue peptide comprising these residues, commonly referred to as M13, has a high affinity ($\sim 10^{-9}$ M) for calcium-loaded CaM. The nature of the interaction between CaM and its targets has been the subject of many biophysical studies.[6–16] However, because of the difficulty in growing X-ray suitable crystals of the CaM–M13 complex, the definitive structure of the complex has not been obtained. Many of the peptides that have a high binding affinity for CaM, including melittin, mastoporan, and a host of synthetic peptides,[17,18] are positively charged and have a propensity to form amphiphilic α-helices. Indeed, circular dichroism studies of CaM complexed with M13 show an increase in α-helicity for the complex compared to Ca^{2+}-loaded CaM, suggesting that the MLCK peptide assumes an α-helical conformation when complexed with CaM.[9] Fluorescence studies of CaM-binding peptides also indicate that a series of peptide analogues form an α-helical conformation when bound to CaM.[19] Small angle X-ray scattering indicates that the CaM–M13 complex is significantly more compact than CaM alone,[16] suggesting a substantial rearrangement in the CaM structure upon binding to M13. Cross-linking studies suggest that the target peptides interact simultaneously with both globular domains of CaM.[17,20]

Previously, we have used triple resonance NMR experiments to obtain complete ^{1}H, ^{13}C, and ^{15}N resonance assignments of CaM in the M13-bound form.[21] Many of these chemical shifts differ substantially from those of free Ca^{2+}-bound CaM. However, with the exception of the middle region of the central helix, NOE measurements indicated no change in secondary structure. These studies required uniform isotopic enrichment of CaM with ^{13}C and ^{15}N, making possible a variety of highly sensitive 3D NMR experiments to obtain resonance assignments and NOE distances. However, no information on the structure of the unlabeled peptide was obtained with these experiments.

Isotopic enrichment of the peptide would permit a range of isotope-edited experiments[22-29] to elucidate its conformation, as

(1) Abbreviations used: CaM, calmodulin; MLCK, myosin light chain kinase; M13, a 26-residue peptide of the CaM-binding domain of rabbit skeletal muscle MLCK comprising residues 577–602; COSY, correlated spectroscopy; NOESY, nuclear Overhauser effect spectroscopy; [F2-N]-NOESY, NOESY with ^{15}N-filtering in F$_2$ dimension; [F1-C,F2-C]-COSY, COSY with ^{13}C-filtering in F$_1$ and F$_2$ dimensions; [F1-C,F2-C]-NOESY, NOESY with ^{13}C-filtering in F$_1$ and F$_2$ dimensions; [F1-C/N,F2-C/N]-NOESY, NOESY with ^{13}C- and ^{15}N-filtering in F$_1$ and F$_2$ dimensions.
(2) Babu, Y. S.; Bugg, C. E.; Cook, W. J. *J. Mol. Biol.* **1988**, *204*, 191–204.
(3) Kretsinger, R. H.; Rudnick, S. E.; Weissman, L. J. *J. Inorg. Biochem.* **1986**, *28*, 289–302.
(4) Ikura, M.; Spera, S.; Barbato, G.; Kay, L. E.; Krinks, M.; Bax, A. *Biochemistry* **1991**, *30*, 9216–9228.
(5) Blumenthal, D. K.; Takio, K.; Edelman, A. M.; Charbonnean, H.; Titani, K.; Walsh, A.; Krebs, E. G. *Proc. Natl. Acad. Sci. U.S.A.* **1985**, *82*, 3187–3191.
(6) For a review, see: Klee, C. B. In *Molecular Aspects of Cellular Regulations*; Cohen, P., Klee, C. B., Eds.; Elsevier: New York, 1988; Vol. 5, pp 35–56.
(7) Jackson, A. E.; Carraway, K. L.; Puett, D.; Brew, K. *J. Biol. Chem.* **1986**, *261*, 12226–12232.
(8) Manalan, A. S.; Klee, C. B. *Biochemistry* **1987**, *26*, 1382–1390.
(9) Klevit, R. E.; Blumenthal, D. K.; Wemmer, D. E.; Krebs, G. E. *Biochemistry* **1985**, *24*, 8152–8157.
(10) Seeholzer, S. H.; Cohen, M.; Putkey, J. A.; Means, A. R.; Crespi, H. I. *Proc. Natl. Acad. Sci. U.S.A.* **1986**, *83*, 3634–3638.
(11) Linse, S.; Drakenberg, T.; Forsen, S. *FEBS Lett.* **1988**, *119*, 28–32.
(12) Ikura, M.; Hasegawa, N.; Aimoto, S.; Yazawa, M.; Yagi, K.; Hikichi, K. *Biochem. Biophys. Res. Commun.* **1986**, *161*, 1233–1238.
(13) Seeholzer, S. H.; Wand, A. J. *Biochemistry* **1989**, *28*, 4011–4020.
(14) Matsushima, N.; Izumi, Y.; Matsuo, T.; Yoshino, H.; Ueki, T.; Miyake, Y. *J. Biochem. (Tokyo)* **1989**, *105*, 883–887.

(15) Kataoka, M.; Head, J. F.; Seaton, B. A.; Engelman, D. M. *Proc. Natl. Acad. Sci. U.S.A.* **1989**, *86*, 6944–6948.
(16) Heidorn, D. B.; Seeger, P. A.; Rokop, S. E.; Blumenthal, D. K.; Means, A. R.; Crespi, H.; Trewhella, J. *Biochemistry* **1989**, *28*, 6757–6764.
(17) O'Neil, K. T.; DeGrado, W. F. *Proteins* **1989**, *6*, 284–293.
(18) O'Neil, K. T.; DeGrado, W. F. *Trends Biochem. Sci.* **1990**, *15*, 50–64.
(19) O'Neil, K. T.; Erickson-Viitanen, S.; DeGrado, W. F. *J. Biol. Chem.* **1989**, *264*, 14571–14578.
(20) Persechini, A.; Kretsinger, R. *J. Biol. Chem.* **1988**, *263*, 12175–12178.
(21) Ikura, M.; Kay, L. E.; Krinks, M.; Bax, A. *Biochemistry* **1991**, *30*, 5498–5504.
(22) Griffey, R. H.; Redfield, A. G. *J. Magn. Reson.* **1985**, *65*, 344–348.
(23) Otting, G.; Senn, H.; Wagner, G.; Wuthrich, K. *J. Magn. Reson.* **1986**, *70*, 500–505.
(24) Senn, H.; Otting, G.; Wuthrich, K. *J. Am. Chem. Soc.* **1987**, *109*, 1090–1092.
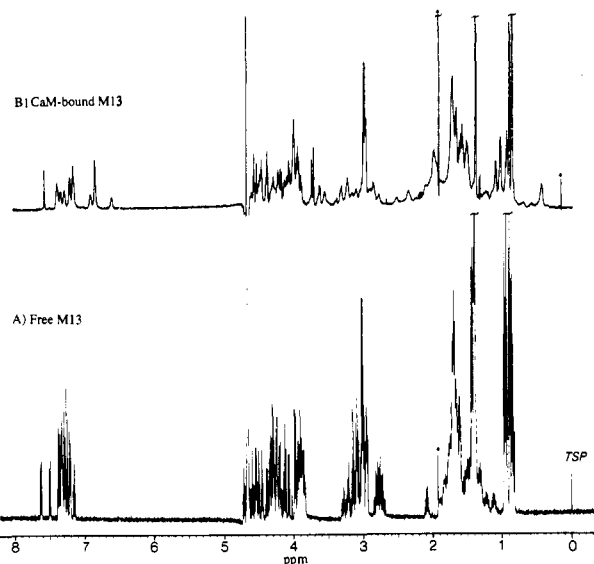(25) Bax, A.; Weiss, M. *J. Magn. Reson.* **1987**, *71*, 571–575.
(26) Fesik, S. W.; Gampe, R. T.; Rockway, T. W. *J. Magn. Reson.* **1987**, *74*, 366–371. Fesik, S. W.; Luly, J. R.; Erickson, J. W.; Abad-Zapatero, C. *Biochemistry* **1988**, *27*, 8297–8301.
(27) Griffey, R. H.; Redfield, A. G. *Q. Rev. Biophys.* **1987**, *19*, 51–82.
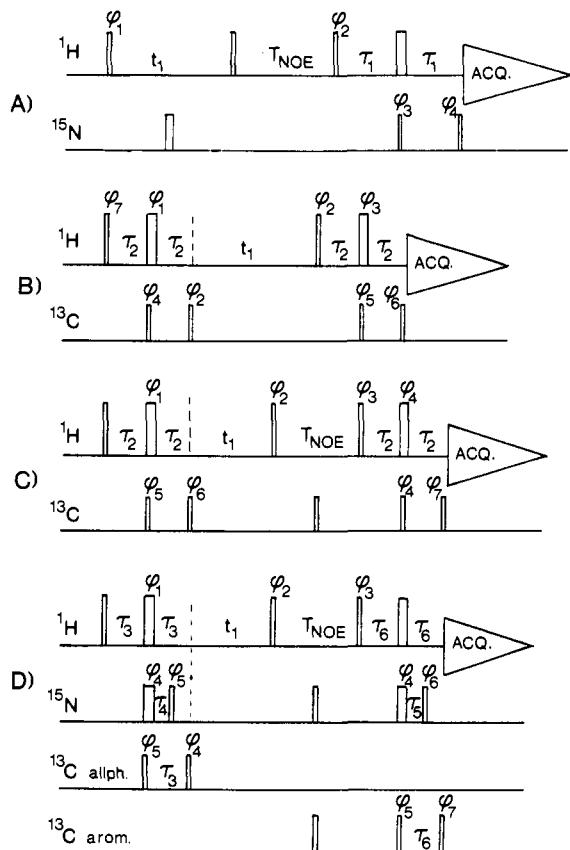
Figure 1. Pulse schemes of (A) the [F2-N]-NOESY experiment, (B) the [F1-C,F2-C]-COSY experiment, (C) the [F1-C,F2-C]-NOESY experiment, and (D) the [F1-C/N,F2-C/N]-NOESY experiment. The latter experiment is optimized to suppress aliphatic resonances in the F_1 dimension and aromatic resonances in the F_2 dimension. In the drawings, wide pulses represent 180° flip angles and narrow pulses have a 90° flip angle. All pulses are applied along the x-axis unless explicitly marked. The phase cycling used is as follows: (A) $\phi_1 = x, -x$; $\phi_2 = 2(x), 2(-y)$, $2(-x), 2(y)$; $\phi_3 = 8(x), 8(-x)$; $\phi_4 = 16(x), 16 (-x)$; Acq. $= x, -x, y, -y$, $-x, x, -y, y$. (B) $\phi_1 = x, y, -x, -y$; $\phi_2 = 4(y), 4(-y)$; $\phi_3 = 8(x), 8(y)$, $8(-x), 8(-y)$; $\phi_4 = 32(x), 32(-x)$; $\phi_5 = 16(x), 16(-x)$; $\phi_6 = 8(x), 8(-x)$; $\phi_7 = x$; Acq. $= 4(x,-x), 4(-x,x)$. (C) $\phi_1 = x, y, -x, -y$; $\phi_2 = x$; $\phi_3 = 4(x), 4(-y), 4(-x), 4(y)$; $\phi_4 = 16(x), 16(-x)$; $\phi_5 = 32(x), 32(-x)$; $\phi_6 = 4(x), 4(-x)$; $\phi_7 = 8(x), 8(-x)$; Acq. $= 2(x,-x), 2(y,-y), 2(-x,x), 2(-y,y)$. (D) $\phi_1 = 8(x,y), 8(-x,-y)$; $\phi_2 = x$; $\phi_3 = x, x, y, y, -x, -x, -y, -y$; $\phi_4 = 16(x), 16(-x)$; $\phi_5 = 8(x), 8(-x)$; $\phi_6 = 4(x), 4(-x)$; $\phi_7 = 48(x), 48(-x)$; Acq. $= x, -x, -y, y, -x, x, y, -y$. The NOE mixing period is marked T_{NOE}, and 90° ($^{13}C/^{15}N$) pulses applied at the midpoint of this interval serve to destroy any residual antiphase z magnetization. Quadrature in the t_1 dimension is achieved using the States–TPPI method, changing phase ϕ_1 in scheme A, phases ϕ_1 and ϕ_7 in concert for scheme B, phase ϕ_2 for schemes C and D. The delay durations used are: $\tau_1 = 5.35$ ms; $\tau_2 = 3.4$ ms; $\tau_3 = 3.5$ ms; $\tau_4 = 1.85$ ms; $\tau_5 = 2.25$ ms; $\tau_6 = 3.1$ ms; $T_{NOE} = 100$ ms.

recently demonstrated most elegantly for cyclosporin A in its complex with cyclophilin.[30,31] However, for ligands such as M13 that are not obtained from microbial sources, uniform isotopic enrichment is prohibitively expensive. As an alternative, at least in principle, one could use uniform ^2H labeling of the protein to allow selective observation of the peptide resonances in the aliphatic portion of the ^1H spectrum.[10] In practice, however, we have been unsuccessful at obtaining sufficient amounts of highly deuterated CaM.
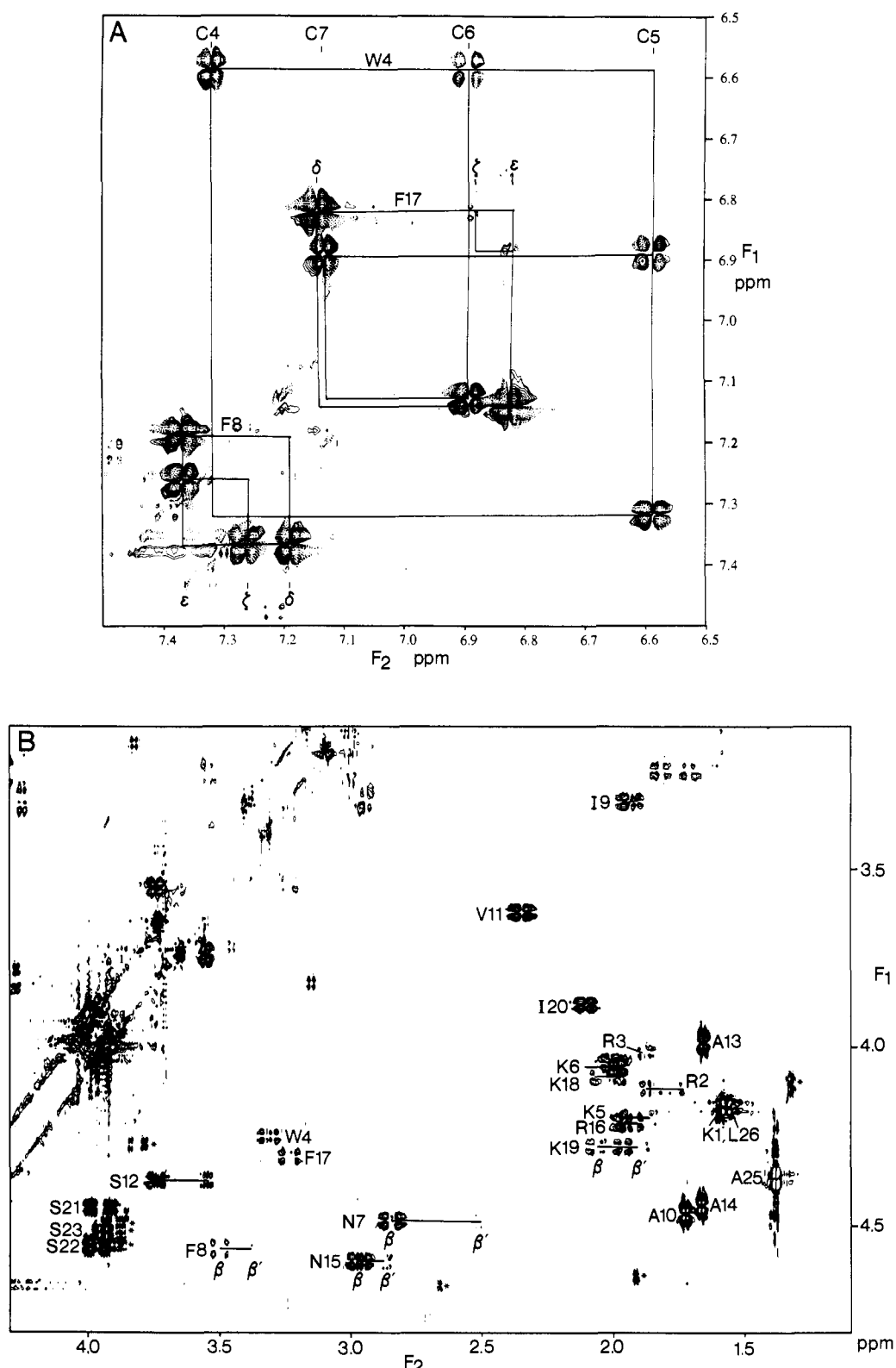
(28) Otting, G.; Wuthrich, K. *Q. Rev. Biophys.* **1990**, *23*, 39–96.

(29) Wider, G.; Weber, C.; Traber, R.; Widmer, H.; Wuthrich, K. *J. Am. Chem. Soc.* **1990**, *112*, 9015–9016.

(30) Weber, C.; Wider, G.; Freyberg, B.; Traber, R.; Braun, W.; Widmer, H.; Wuthrich, K. *Biochemistry* **1991**, *30*, 6563–6574.

(31) Fesik, S. W.; Gampe, R. T.; Eaton, H. L.; Gemmecker, G.; Olejniczak, E. T.; Neri, P.; Holzman, T. F.; Egan, D. A.; Edalji, R.; Simmer, R.; Helfrich, R.; Hochlowski, J.; Jackson, M. *Biochemistry* **1991**, *30*, 6574–6583.

Figure 2. 1D ^1H NMR spectra of (A) free M13 and (B) M13 bound to [$^{13}C,^{15}N$]-labeled CaM, recorded in D_2O solution. Protein resonances are suppressed in spectrum B, and it has been recorded using the [F1-C,F2-C]-COSY sequence of Figure 1B with t_1 set to zero. The resonance marked with an asterisk originates from an impurity.

Here we demonstrate that doubly isotope-filtered experiments can be used as an alternative method for observing the peptide signals selectively and that spectra are of sufficient quality to derive structural information.

Experimental Procedures

Sample Preparation. *Drosophila* CaM was overexpressed by using the pAS vector in *Escherichia coli* (strain AR58), using the M9 minimal medium, containing 3 g/L of [$^{13}C_6$]glucose and 1 g/L of [^{15}N]NH$_4$Cl. A 2.4-L preparation yielded 18 mg of purified [$^{15}N,^{13}C$]-labeled CaM, sufficient for two NMR samples. In addition, a protein preparation labeled with ^{15}N only was made, resulting in 20 mg of uniformly ^{15}N-labeled CaM. The protein purification procedure has been described previously.[32] Chemically synthesized HPLC purified peptide M13 (KRRWKKNFIAVSAANRFKKISSSGAL) (Peptide Technologies Corp. Washington, DC) was used without further purification. NMR samples of the M13–CaM complex were prepared according to the procedure outlined by Seeholzer and Wand.[13] The pH of both the H$_2$O sample (1.4 mM in 95% H$_2$O, 5% D$_2$O) and the D$_2$O sample (1.0 mM in 99.9% D$_2$O) was adjusted to 6.8 (uncorrected meter reading). In addition, a 1.5-mM sample of uniformly ^{15}N-labeled CaM/M13 complex was prepared, also at pH 6.8.

NMR Spectroscopy. All NMR experiments were carried out on a Bruker AM-600 and a Bruker AMX-600 NMR spectrometer, both operating at 600 MHz, 35 °C, and both equipped with triple resonance hardware. The 2D NMR experiments carried out employ isotope filtering to select resonances from protons not attached to ^{13}C or ^{15}N. All NOESY experiments were carried out with a 100-ms NOE mixing period and a 1.1-s relaxation delay between scans. For the H$_2$O experiments, presaturation of the H$_2$O resonance was used during the relaxation delay time between scans, using a presaturating field of ~30 Hz. As a shorthand notation, we use [F1-C/N,F2-N] to indicate that in the F_1 dimension protons attached either to ^{13}C or to ^{15}N are suppressed, and in the F_2 dimension resonances of ^{15}N attached protons are suppressed. The [F2·N]-NOESY spectrum results from a 800 (real) × 2048 (real) data matrix with acquisition times of 56 ms (t_1) and 123 ms (t_2), using 64 scans per t_1 increment. For the [F1-C/N,F2-C/N]-NOESY experiment a 300 (complex) × 512 (complex) matrix was acquired with acquisition times of 48 ms (t_1) and 73 ms (t_2) and 192 scans per complex increment. The [F1-C,F2-C]-NOESY experiment was carried out using a 350 (complex) × 1024 (complex) matrix with acquisition times of 65 ms (t_1) and 170 ms (t_2), using 192 scans per complex t_1 increment. Finally, the [F1-C,F2-C]-COSY spectrum resulted from a 512 (complex) × 1024 (complex) matrix with acquisition times of 95 ms (t_1) and 170 ms (t_2), and 128 scans per complex t_1 increment. For data processing of the COSY data, diagonal subtraction[34] was used to obtain a phase-

(32) Ikura, M.; Marion, D.; Kay, L. E.; Shih, H.; Krinks, M.; Klee, C. B.; Bax, A. *Biochem. Pharmacol.* **1990**, *40*, 153–160.

2D NMR of a Protein-Peptide Complex

*J. Am. Chem. Soc., Vol. 114, No. 7, 1992* 2435

Figure 3. Two sections of the phase-sensitive [F1-C,F2-C]-COSY spectrum of the M13–CaM complex recorded in D_2O solution. The dispersive diagonal has been subtracted from the spectrum using a routine described by Pelczer:[34] (A) aromatic region, (B) aliphatic region. Cross peaks marked by asterisks (*) originate from a slight excess of free M13 peptide.

sensitive spectrum with optimal sensitivity. For all NOESY spectra, 45° shifted sine bell filtering was used in the F_1 dimension and 60° shifted sine-squared bell filtering in the F_2 dimension. For the COSY spectrum, 15° shifted sine bell filtering was used in both dimensions. The total measuring time was ~22 h for each of the 2D spectra.

Results and Discussion

The pulse sequences used in the present work are shown in Figure 1. The schemes are simple extensions of isotope-filtering

schemes described earlier.[23-29] However, since in the present work the focus is on analyzing the data of the nonlabeled component of the complex, particular care needed to be taken to minimize filtration artifacts. Although isotope-filtered (with isotope attached protons suppressed) and isotope-edited data (with isotope attached resonances selected) can be obtained from the same sets of data by judiciously making linear combinations of data acquired separately,[29] we found the quality of the isotope-filtered data obtained
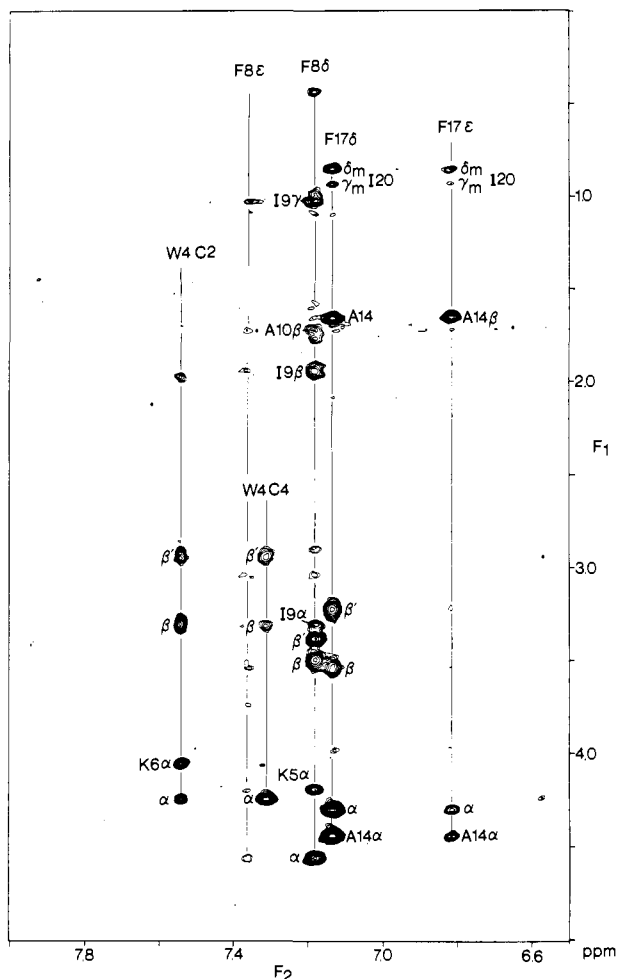
Figure 4. The aromatic/aliphatic cross-peak region of the [F1-C,F2-C]-NOESY spectrum of M13–CaM recorded in D_2O solution, recorded with the scheme of Figure 1C.

Table I. Proton Resonance Assignments of the 26-Residue Myosin Light Chain Kinase Peptide (M13) Bound to Calmodulin at 35 °C and pH 6.8[a]

| residue	HN	$C_\alpha H$	$C_\beta H$	other
K1	b	4.17	1.57, 1.57	b
R2	b	4.12	1.85, 1.76	b
R3	7.52	4.02	2.06, 1.97	b
W4	8.11	4.25	3.31, 2.94	C_2H 7.55; C_4H 7.32; C_5H 6.59; C_6H 6.89; C_7H 7.13; NH 10.29
K5	8.16	4.19	1.94, 1.89	b
K6	8.64	4.05	2.00, 2.00	b
N7	7.45	4.49	2.84, 2.51	
F8	8.91	4.57	3.50, 3.38	$C_\delta H$ 7.19; $C_\epsilon H$ 7.37; $C_\zeta H$ 7.27
I9	9.17	3.31	1.94	$C_{\gamma m}H$ 1.03; $C_\gamma H$ 1.95, 1.00; $C_\delta H$ 0.43
A10	8.06	4.47	1.72	
V11	8.29	3.61	2.35	$C_{\gamma m}H$ 1.10, 1.03
S12	8.72	4.38	3.74, 3.55	
A13	9.05	3.99	1.66	
A14	8.44	4.45	1.67	
N15	8.35	4.60	2.96, 2.88	NH_2 8.43, 5.40
R16	8.28	4.21	1.96, 1.92	b
F17	8.69	4.31	3.54, 3.22	$C_\delta H$ 7.15; $C_\epsilon H$ 6.83; $C_\zeta H$ 6.89
K18	7.81	4.09	2.05, 1.99	$C_\gamma H$ 1.52; $C_\delta H$ 1.67; $C_\epsilon H$ 2.98
K19	7.70	4.21	1.95, 1.95	b
I20	8.07	3.88	2.11	$C_{\gamma m}H$ 0.93; $C_\gamma H$ 1.72, 1.11; $C_\delta H$ 0.85
S21	7.83	4.45	3.99, 3.92	
S22	8.13	4.56	4.00, 3.94	
S23	8.30	4.52	3.97, 3.93	
G24	8.28	b		
A25	7.96	4.37	1.38	
L26	7.78	4.16	1.56, 1.56	$C_\gamma H$ 1.62; $C_\delta H$ 0.90, 0.87

[a] Chemical shifts are expressed in ppm relative to (trimethylsilyl)-propionic-d_4 acid (TSP) and measured with respect to the water resonance which has a chemical shift of 4.67 ppm at 35 °C. [b] Assignment not obtained.

this way to be much lower than those of the isotope-selected counterpart. Therefore, we have used isotope-filtering procedures based on purge pulses,[33] which in our hands result in cleaner spectra. Moreover, isotope-edited 2D NOESY spectra for studying the interaction between the peptide and the protein are not needed since these spectra can be acquired advantageously in a 3D manner, using the ^{13}C or ^{15}N shift of the protein to separate these interactions. The mechanism of purge filters in terms of operator formalism has been given previously[33] and will not be repeated here.

Figure 2 compares the spectrum of the free M13 peptide in D_2O solution with the ^{13}C-filtered 1D spectrum of the CaM–M13 complex. The free M13 spectrum is characteristic of an unstructured "random coil" peptide. The isotope-filtered spectrum of the complex shows substantial chemical shift changes in the ^1H NMR spectrum and a large increase in line width for the individual resonances, which is expected because of the slower molecular tumbling of the 20-kDa molecular complex. The isotope-filtered 1D spectrum results from using the [F1-C,F2-C]-COSY pulse sequence of Figure 1B, with t_1 set to zero.

Figure 3 shows two sections of the phase-sensitive [F1-C,F2-C]-COSY spectrum of the M13–CaM complex. Note that the dispersive diagonal has been subtracted from this spectrum using a routine described by Pelczer.[34] In the aromatic region of the spectrum (Figure 3A), signals for the tryptophan and the two phenylalanine residues can be identified. The Phe Hδ protons and Trp C4H are easily distinguished from other aromatic ring

protons by their intense intra-residue NOE cross peaks with their intra-residue Hα and Hβ resonances in the [F1-C,F2-C]-NOESY spectrum (Figure 4). The aliphatic region of the [F1-C,F2-C]-COSY spectrum (Figure 3B) shows the Hα–Hβ cross peaks and permits identification of the type of amino acid for a substantial fraction of the residues. For example, the single valine and all four serine and four alanine residues are immediately recognized. Both phenylalanine residues and the tryptophan are recognized by comparing their Hα–Hβ cross peaks with the NOE cross peaks to their aromatic rings (Figure 4). Although the M13 peptide consists of only 26 amino acids, its assignment is made more difficult by the fact that the M13 proton line widths correspond to that of a 20-kDa protein. As a consequence, most of the Hα–Hβ cross peaks for J values smaller than ~5 Hz are missing in the [F1-C,F2-C]-COSY spectrum. Therefore, typically Hα shows nonvanishing J cross peaks to only a single Hβ proton, except for residues that have considerable mobility about their χ_1 angle. Residues for which intense J cross peaks from Hα to both Hβ protons are observed are mainly located at the C-terminus of the peptide and include residues S21, S22, and S23. The chemical shifts of M13 in the complex with CaM are summarized in Table I.

Figure 5 compares the amide/aliphatic cross-peak region of the NOESY spectrum recorded (A) without any filtering, (B) with [F2-N] editing, and (C) with [F1-C/N,F2-C/N] filtering. Clearly, the regular NOESY spectrum (Figure 5A) is far too crowded for a detailed analysis. The [F2-N]-NOESY spectrum (Figure 5B) allows a large number of cross peaks to be identified for each of the peptide amide protons. Note that interactions with aromatic protons in the protein are also present in this spectrum and that this spectrum does not distinguish intermolecular from intramolecular interactions. The doubly edited [F1-C/N,F2-C/N] spectrum (Figure 5C) allows this distinction to be made and immediately identifies a large number of intrapeptide NOE interactions. Note, however, that, because of the slightly longer delays and the additional 180° ^1H pulse needed for the scheme of Figure 1D, the sensitivity of the doubly-filtered experiment is

(33) Kogler, H.; Sorensen, O. W.; Ernst, R. R. *J. Magn. Reson.* **1983**, *55*, 157–163.

(34) Pelczer, I. *J. Am. Chem. Soc.* **1991**, *113*, 3211–3212.
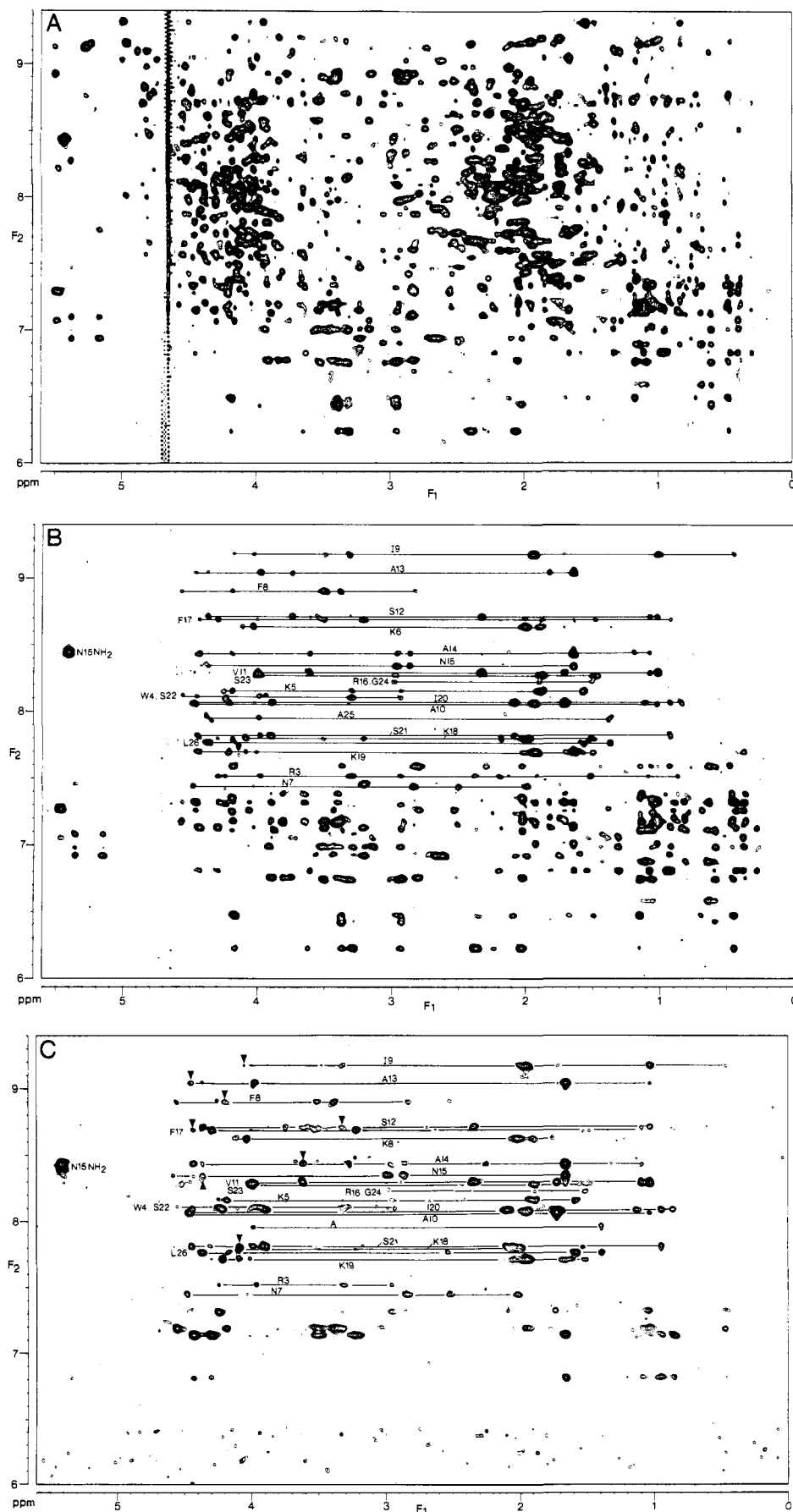
Figure 5. The amide/aliphatic cross-peak region of the NOESY spectrum recorded on the M13–CaM complex in H_2O solution (A) without any filtering, (B) with [F2-N] filtering (using the pulse scheme of Figure 1A), and (C) with [F1-C/N,F2-C/N] filtering (using the pulse scheme of Figure 1D). In panel B, both inter- and intramolecular NOE interactions to the peptide amides are present, as well as inter- and intramolecular interactions to both the amide and the protein aromatic protons. In panel C, only intramolecular NOE interactions involving the peptide amide protons and the aromatic peptide protons (in the F_2 = 7.3–6.8 ppm region) are present. Correlations marked by arrowheads in panel (C) correspond to $d_{\alpha N}(i,i+3)$ connectivity.

somewhat lower than for the [F2-N] spectrum.

The doubly-filtered [F1-N/C,F2-N/C] NOE spectrum of Figure 5C has been recorded with the pulse scheme of Figure 1D. This pulse scheme has been designed to provide a compromise between the required filtering efficiency and high signal-to-noise. Because the ^{15}N-attached protons are filtered twice (once preceding t_1 and once preceding t_2) using a single-step purge filter (each providing typically ~85% suppression of the ^{15}N-attached proton signals), the protein diagonal amide resonances and amide–amide cross peaks are suppressed nearly 50-fold. Cross peaks from aliphatic CaM resonances (t_1) to M13 amide resonances are suppressed by a ^{13}C two-step purge filter preceding the t_1 period. Because of the relatively large range of $^1J_{CH}$ coupling constants (125–155 Hz), a uniformly high level of suppression of these cross peaks cannot be obtained for all aliphatic protons simultaneously with a single purge pulse. However, because a 5.35-ms delay (τ_3 + τ_4) is used for the ^{15}N filter, an additional delay of only 1.65 ms is needed to apply the two-step ^{13}C purge filter, used in the scheme of Figure 1D. Note that the purge filter preceding t_1 is applied with the ^{13}C carrier in the center of the aliphatic resonances. To remove aromatic CaM signals that might be obscuring M13 amide signals, the t_2 detection period is preceded by a two-step ^{13}C purge filter with the ^{13}C carrier set to the center of the aromatic resonances. Purging of the aromatic protein signals also reveals the intramolecular interactions for the aromatic resonances of the M13 peptide. Note, however, that higher quality data for these interactions can be observed in the [F1-C,F2-C]-NOESY spectrum recorded in D$_2$O, shown in Figure 4.

Comparison of the [F1-N/C,F2-N/C] spectrum (Figure 5C) with the [F2-N]-NOESY spectrum (Figure 5B) indicates that none of the resonances remaining in Figure 5C are significantly attenuated relative to Figure 5B, and therefore the remaining cross peaks all must correspond to intramolecular peptide NOEs. The [F2-C] double-purge filter of Figure 1D is adjusted to minimize signals from aromatic protein protons by switching the ^{13}C carrier frequency from the aliphatic to the aromatic region of the spectrum. This frequency switching was necessary because, at the time these experiments were conducted, our triple resonance probe had insufficient ^{13}C efficiency to provide an accurate 90° pulse across the entire spectral width (requiring a ~25-kHz rf field). Also, because the aromatic ^{1}H–^{13}C couplings (~160 Hz) are larger than the aliphatic couplings, shorter purge delays (3.1 ms) are used. The double [F2-C] filter provides excellent suppression of the aromatic protein resonances. This was particularly important to identify the potential presence of slowly exchanging side-chain protons of the asparagine and arginine residues of the peptide. Only one such resonance is observed in the spectrum of Figure 5C, corresponding to the Asn-15 side chain. The side-chain amide protons of this residue resonate at unique well-separated chemical shifts, 8.43 and 5.40 ppm. This assignment was based on the intra-residue NOEs between the amide protons and the Hβ protons. The chemical shift difference between the two side-chain NH$_2$ protons (3.03 ppm) is unusually large. However, the NOE spectra do not show interactions of these peaks with aromatic peptide or protein resonances, suggesting that the unusual chemical shifts cannot be attributed to ring-current effects. Relatively strong NOE interactions between the most upfield of the two NH$_2$ protons and aliphatic signals at 1.08, 1.19, 2.13, and 4.19 ppm are marked in the [F2-N]-NOESY spectrum shown in Figure 6, and these resonances have been tentatively assigned to Ile-85, C$_\gamma$H′, C$_\gamma$H$_3$, C$_\gamma$H″, and C$_\alpha$H, located in the C-terminal half of the "central helix". Weaker NOE cross peaks between the other Asn-15 NH$_2$ proton (overlapping with Ala-14 NH) and these aliphatic protein resonances are also observed, suggesting that the side chain is embedded in a hydrophobic environment. Further 3D NOE studies are in progress to detail the nature of the interaction between the Asn-15 NH$_2$ moiety and CaM.

The highest quality of the NH–NH connectivity region was obtained with the sequence of Figure 1A, using the sample with ^{15}N (and no ^{13}C) labeled protein. The pertinent region of the [F2-N]-NOESY spectrum is shown in Figure 7. A long chain of d_{NN} connectivities, from Arg-3 to Ser-22, is observed, indicating
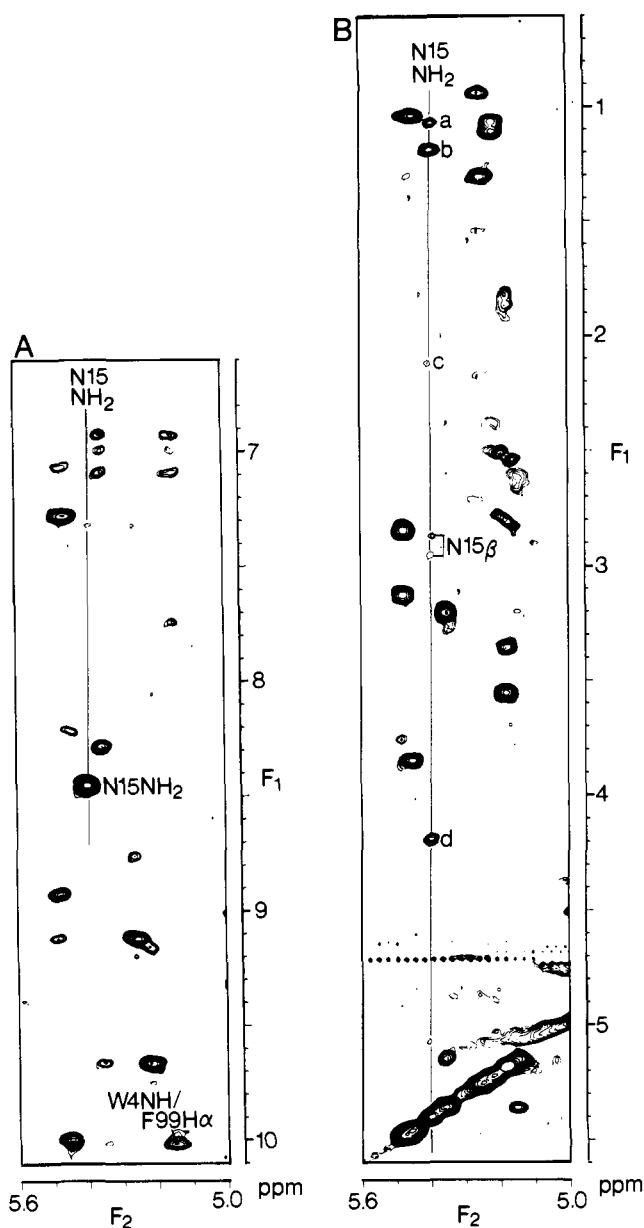

Figure 6. Selected regions of the [F2-N]-NOESY spectrum of M13–CaM recorded in H$_2$O solution, showing the NOE interactions observed for the upfield side-chain amide proton of Asn-15. Quadrature in the t_1 dimension is achieved using TPPI. Note that the ring NH proton of Trp-4 is folded in the F$_1$ dimension and its true chemical shift is 10.29 ppm. Cross peaks between the upfield Asn NH$_2$ resonance (5.40 ppm) and aliphatic protein resonances (tentatively assigned to Ile-85) are marked "a", "b", "c", and "d".

a helical conformation of M13 when bound to CaM. A weak intermolecular interaction between Ile-9 NH of M13 and Tyr-138 Hδ of CaM is also marked in this figure. An interaction between the Trp-4 side-chain NH proton and Phe-99 Hα falls outside the region shown in Figure 7, but can be clearly seen in Figure 6. In total 133 such intermolecular NOEs have been identified, largely by 3D isotope-filtered techniques. Analysis of these intermolecular contacts is presently in progress and will be discussed elsewhere.

To ascertain that M13 adopts an α-helical conformation when bound to CaM, it is important to analyze the aliphatic region of the NOESY spectrum which should show significant $d_{\alpha\beta}(i,i+3)$ connectivities for an α-helix. Indeed, numerous such NOEs are observed in the region of the [F1-C,F2-C]-NOESY spectrum shown in Figure 8. Further confirmation of the α-helical geometry is found in a large number of $d_{\alpha N}(i,i+3)$ connectivities in the spectrum of Figure 5C. The short-range NOEs observed for the M13 peptide are summarized in Figure 9 and indicate an α-helical

2D NMR of a Protein–Peptide Complex

J. Am. Chem. Soc., Vol. 114, No. 7, 1992 2439
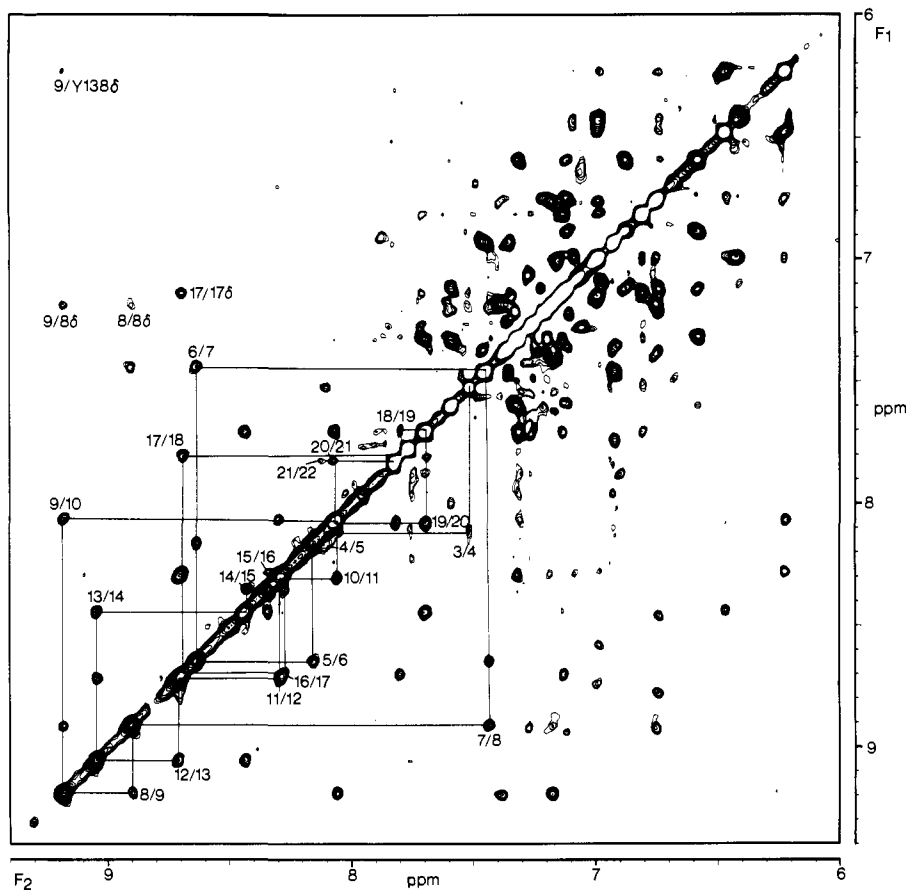
Figure 7. The amide region of the [F2-N]-NOESY spectrum recorded on the M13-[^{15}N]-labeled CaM in H_2O solution. A stretch of d_{NN} connectivities from Arg-3 to Ser-22 is indicated. A weak intermolecular interaction between Ile-9 HN of M13 and Tyr-138 Hδ of CaM is also marked.
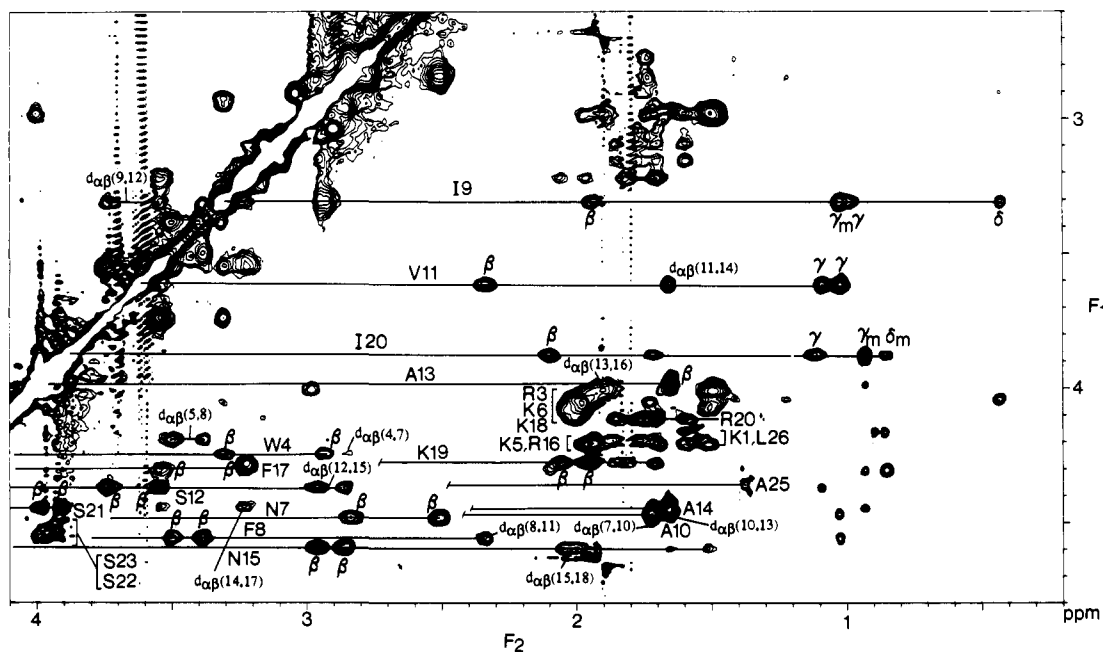

Figure 8. The aliphatic region of the [F1-C,F2-C]-NOESY spectrum of M13–CaM, recorded in D_2O solution. Intra-residue and $d_{\alpha\beta}(i,i+3)$ connectivities are marked.

conformation for the peptide starting at Arg-3 and continuing through Ser-21. The M13 amide protons of residues Lys-1 and Arg-2 could not be identified, presumably because of rapid exchange with solvent. The side chain of the N-terminal peptide residue shows narrow resonances in the NMR spectrum and is presumably highly mobile. The Arg-2 side-chain Hα/Hβ cross peaks observed in Figure 3 are weak, suggesting that this side chain is not freely rotating. The C-terminal residues 23 to 26 do not

show any characteristic α-helical NOE patterns such as d_{NN}-$(i,i+1)$, $d_{\alpha N}(i,i+3)$, or $d_{\alpha\beta}(i,i+3)$ connectivities, and they exhibit relatively intense cross peaks in the COSY spectrum, suggesting mobility in the C-terminus.

Early NMR studies[9,11,12] showed spectral changes in both globular domains of CaM upon complexation with peptide, and cross-linking studies[20] confirmed that the peptide interacts with both domains simultaneously. These results, combined with the
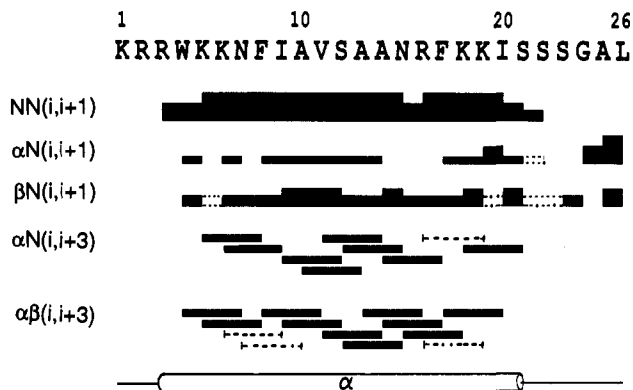
Figure 9. Amino acid sequence of the MLCK peptide (M13) and summary of the short-range NOEs involving HN, CαH, and CβH protons together with the secondary structure deduced from these data. NOEs that are presumably present but which cannot be identified because of resonance overlap are indicated with broken lines.

present study, which indicates that the conformation of the M13 peptide is α-helical when bound to CaM, show that the "central helix" of CaM cannot exist as a single straight helix in its complex with target peptide, because the α-helical peptide is too short to interact with both domains simultaneously. The "central helix" of M13-complexed CaM therefore must bend in order to bring the two globular domains sufficiently close together. The change in molecular shape that accompanies complexation has previously been observed using small angle X-ray scattering.[14-16]

Based on molecular modeling studies, Persechini and Kretsinger[35] reported that the two domains of CaM can easily interact with a helical cylinder-type peptide if one allows only a single kink in the "central helix" by altering the ψ torsion angle of Ser-81. A more recent NMR study[21] indicates a change in the NOE patterns in the "central helix" for residues Lys-75 through Ser-81 upon complexation with M13, suggesting that the disruption of the central helix is more extensive than in the simple Persechini

and Kretsinger model. The intermolecular interaction between M13 Ile-9 NH and CaM Tyr-138 Hδ seen in Figure 7 and the NOE between the side chain of M13 Trp-4 and Hα of CaM Phe-99 (Figure 6) suggest that the peptide is aligned in an antiparallel fashion relative to the protein; i.e., the N-terminal end of M13 interacts with the C-terminal domain of CaM. A number of other NOEs, including several between Phe-17 of M13 and Ile-27 of CaM, confirm that the alignment is antiparallel. This orientation of the peptide helix is opposite to that in the model of Persechini and Kretsinger[35] but agrees with the results of cross-linking experiments by O'Neil and DeGrado.[17]

The structure determination of the CaM–M13 complex based on our NMR data is currently in progress and will be reported elsewhere. Whether the MLCK binding site has an α-helical conformation in the intact protein or exists as an unstructured large loop prior to CaM binding is not clear from the present study. To address this question it will be necessary to examine a larger folded domain of the target protein.

The methodology presented here for studying the conformation of a bound ligand is particularly useful when isotopically enriched protein is available, whereas isotopic enrichment of the ligand is prohibitively expensive. Note that even if isotopically labeled ligand could be obtained, isotopic enrichment of the receptor protein generally will be needed anyway to investigate in detail the interaction between ligand and receptor. Therefore, the isotope-filtering experiments described here are generally useful for the study of the ligand in a protein–ligand complex, prior to the study of the ligand–protein interactions.

Registry No. MLCK, 51845-53-5; M13, 99268-57-2.

(35) Persechini, A.; Kretsinger, R. J. Cardiovas. Pharmacol. (S5) 1988, 12, 1-12.

Stable Polarons in Polyacetylene Oligomers: Optical Spectra of Long Polyene Radical Cations

Thomas Bally,*,† Kuno Roth,† W. Tang,† Richard R. Schrock,‡ Konrad Knoll,‡ and Lee Y. Park‡

Contribution from the Institut de Chimie Physique, Université de Fribourg, Pérolles, CH-1700 Fribourg, Switzerland, and Department of Chemistry, Massachusetts Institute of Technology, Cambridge, Massachusetts 02139. Received September 23, 1991

Abstract: The radical cations of tert-butyl-capped polyenes containing 3–13 conjugated double bonds were generated radiolytically in Freon matrices and investigated by electronic absorption spectroscopy. The observed spectra are in accord with a qualitative MO/CI model which predicts two bands of disparate intensity which both undergo a shift to lower energies as the chain grows longer. Extrapolation to infinite chain length leads to an energy of ~0.4 eV for the second, intense band and ~0.1 eV for the first, weak band. This finding and its implications with regard to the structure of polarons in polyenes and the nature of doped and/or photoexcited polyacetylene are discussed.

1. Introduction

The primary species obtained upon *doping* of polyacetylene $(CH)_x$ are radical cations or radical anions (called polarons P^+/P^- in the language of solid-state physics).[1] The role of these primary species in the conduction mechanism of doped $(CH)_x$ is somewhat

elusive because at moderate dopant levels, the concentration of spins is too low to account for the observed conductivities in terms

* To whom correspondence should be addressed.
† University of Fribourg.
‡ Massachusetts Institute of Technology.

(1) Many excellent reviews and monographs have recently been published on the topic of conducting polymers and the theoretical models used to explain their behavior. The presently relevant case of polyacetylene receives special attention in (a) Roth, S.; Bleier, H. Adv. Phys. 1987, 36, 2385. (b) Heeger, A. J.; Kivelson, S.; Schrieffer, J. R.; Su, W.-P. Rev. Mod. Phys. 1988, 60, 781. (c) Baeriswyl, D.; Campbell, D. K.; Mazumdar, S. In The Physics of Conducting Polymer; Kiss, H., Ed.; Springer: Berlin, 1992.